Synthesis, characterization and comparative study of thiophene–benzothiadiazole based donor–acceptor–donor (D–A–D) materials†

Prashant Sonar,*[a] Samarendra P. Singh,*[a] Philippe Leclère,[b] Mathieu Surin,[b] Roberto Lazzaroni,[b] Ting Ting Lin,[a] Ananth Dodabalapur[ac] and Alan Sellinger‡[a]

Received 17th November 2008, Accepted 18th February 2009
First published as an Advance Article on the web 25th March 2009
DOI: 10.1039/b820528k

The synthesis and characterization of solution processable donor–acceptor–donor (D–A–D) based conjugated molecules with varying ratios of thiophene as donor (D) and benzothiadiazole as acceptor (A) are reported. Optical, electrochemical, thermal, morphological and organic thin film transistor (OTFT) device properties of these materials were investigated. The thermal and polarized optical microscope analysis indicates that the materials having higher D/A ratios exhibit both liquid crystalline (LC) and OTFT behavior. AFM analysis of the materials having D/A ratios of 3 and 4 (**3T1B** and **4T1B**) show well ordered structures, resulting from strong π–π interchain interactions compared to the other molecules in this study. A XRD patterns for **3T1B** and **4T1B** thin films also shows high crystalline ordering. Solution processed OTFTs of **3T1B** and **4T1B** have shown un-optimized charge carrier mobilities of 2×10^{-2} cm^2 V^{-1} s^{-1} and 4×10^{-3} cm^2 V^{-1} s^{-1}, respectively on bare Si/SiO$_2$ substrate.

1. Introduction

Conjugated semi-conducting materials have been the focus of intense research over the last two decades as they exhibit a variety of interesting optical, electrochemical, morphological and electrical properties.[1] For example, active thin layers on the order of 10–100 nm of such materials can be applied in various electro-optical devices such as organic light emitting diodes (OLEDs),[2] organic photovoltaic devices (OPVs)[3,4] and organic thin film transistors (OTFTs).[5] These materials are promising for such devices as they meet the prerequisite of charge transporting properties, band-gap energy, and light absorption/emission characteristics. Among these materials, conjugated molecules can be more desirable than polymers due to properties such as straightforward purification methods, high purity, simple processing (spin coating, printing, and evaporation) and ample scope for structural modification that makes them promising candidates for electronic devices.[6,7] Over the past few years, an extensive range of functionalized π-conjugated materials have been designed and synthesized with desirable opto-electronic properties.[1] Of these materials, low band gap conjugated materials are of interest because of their high tendency for harvesting visible wavelength photons, tunable red-ox and utility in ambipolar transistors.[8,9] Additionally this system enhances the intramolecular charge transfer which can promote charge carrier mobility.[10] An important property to this end is the modulation of the HOMO–LUMO (highest occupied molecular orbital–lowest unoccupied molecular orbital) gap of conjugated molecules, which can be simply achieved by introducing suitable electron donor and acceptor (D/A) functional groups within the molecule.[11–13] In such systems, interactions of the HOMO of the electron donating (D) and the LUMO of the electron accepting (A) moiety causes the reduction of the band gap of these materials.[14–16] The opto-electronic properties of organic molecules composed of donor and acceptor moieties can be manipulated by systematic control of the numbers of donors and acceptors moieties within the molecules. A key characteristic of these novel semi-conductors is that these types of materials can assist manipulation of electronic structures and crystallinity.[17,18] Although the D–A–D approach in organic materials have been systematically studied for tuning the optical properties, there are very few examples reported on the electrical properties and their application in organic devices.[19–21] Contrary to D–A–D molecules recently A–D–A kind of compounds are also synthesized and investigated for OTFT applications.[22] In such molecular systems, it could be an interesting study to evaluate the electrical properties with respect to the D : A ratio within the D–A–D or A–D–A materials. One potential limitation is that most alkyl free organic semi-conducting materials have very limited solubility in organic solvents, which makes solution processing virtually impossible. To truly realize the advantage of these materials for solution processable devices, alkyl substitution is necessary.[23] Furthermore, symmetrical or asymmetrical alkyl substitution may help to induce highly ordered smectic mesophases in such

[a]*Institute of Materials Research and Engineering (IMRE), The Agency for Science, Technology and Research (A*STAR), 3 Research Link, Singapore, 117602, Republic of Singapore. E-mail: sonarp@imre.a-star.edu.sg; samar-singh@imre.a-star.edu.sg*
[b]*Université de Mons-Hainaut, Service de Chimie des Matériaux Nouveaux, Place du Parc 20, B-7000 Mons, Belgium*
[c]*Microelectronics Research Center, University of Texas at Austin, Austin, TX, 78758, USA*

† Electronic supplementary information (ESI) available: MALDI-TOF spectra, NMR spectra, cyclic voltammograms, DSC thermographs, polarizing optical micrographs, TGA spectra and XRD patterns. See DOI: 10.1039/b820528k

‡ Current address: Department of Materials Science and Engineering and the Center for Advanced Molecular Photovoltaics (CAMP), Geballe Laboratory for Advanced Materials, 476 Lomita Mall, Stanford University, Stanford, CA 94305-4045, USA.

materials.[24] Such behaviour in organic thin films may be advantageous as it supports morphological reorganization which may enhance the effective charge transport.[25]

In this study we have designed and synthesized materials having benzothiadiazole as an acceptor and thiophene as donor moieties with hexyl/octyl chains for solubility. The benzothiadiazole group has been selected in many systems as it acts as both an electron transporting and highly fluorescent chromophore.[26–29] Additionally, the link of benzothiadiazole with thiophene segments represent a useful material combination resulting in red shifted UV-vis and emission spectra compared to equivalent oligothiophenes. Apart from this, the sulfur–nitrogen (S–N) interactions within these molecules may lead to unique molecular assemblies.[20] The molecules reported here are red to orange emitters with optical band gap in the range of 1.95–2.22 eV. Additionally, optical, electrochemical, thermal, morphological and thin film transistor properties of these D–A–D materials were studied. Preliminary results demonstrate OTFTs made from **3T1B** and **4T1B**[30,31] on bare Si/SiO_2 with mobilities of 2×10^{-2} and 4×10^{-3} cm^2 V^{-1} s^{-1} respectively using solution based deposition of the semi-conducting material.

2. Results and discussion

2.1 Synthesis and characterization

The structures of the target compounds **4T1B** (four thiophene with one benzothiadiazole), **3T1B** (three thiophene with one benzothiadiazole), **2T2B** (two thiophene with two benzothiadiazole) and **2T1B** (two thiophene with one benzothiadiazole) are illustrated in Scheme 1. **4T1B** and its detailed synthesis are reported elsewhere.[31] **3T1B**, **2T2B** and **2T1B** materials are reported here for the first time (to the best of our knowledge) and were synthesized using Suzuki and Stille coupling routes. In this manuscript we are reporting the synthesis and characterization of **3T1B**, **2T2B** and **2T1B** materials and their comparative study with **4T1B**.

As shown in Scheme 2, the starting material 2-tributylstannyl-5-octylthiophene (**2**) was first synthesized from 5-octylthiophene (**1**) by selectively lithiating at the 5-position using *n*-butyllithium followed by reacting with tributyl tin chloride using known procedures. 4-(5-octylthiophen-2-yl)benzo[c][1,2,5]thiadiazole (**3**) was synthesized in 65% yield by Stille coupling using one equivalent of 4-bromobenzo[c][1,2,5]thiadiazole with an excess

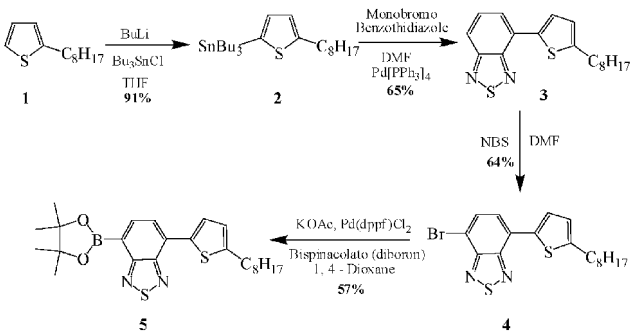

Scheme 2 Synthesis of the thiophene–benzothiadiazole precursors.

of 2-tributylstannyl-5-octylthiophene (**2**) (1.5 eqv.) using $Pd(PPh_3)_4$ as a catalyst in DMF solvent. 4-Bromo-7-(5-octylthiophen-2-yl)benzo[c][1,2,5]thiadiazole (**4**) was then obtained from compound **3** by bromination using *N*-bromosuccinimide (NBS) in a DMF/chloroform solvent mixture at 60 °C for two days. 4-(4,4,5,5-Tetramethyl-1,3,2-dioxaborolan-2-yl)-7-(5-octylthiophen-2-yl)benzo[c][1,2,5]thiadiazole (**5**) was prepared from compound **4** by using bis(pinacolato)diboron, $[PdCl_2(dppf)]$ (dppf = 1,1′-bis(diphenylphosphino)ferrocene) as

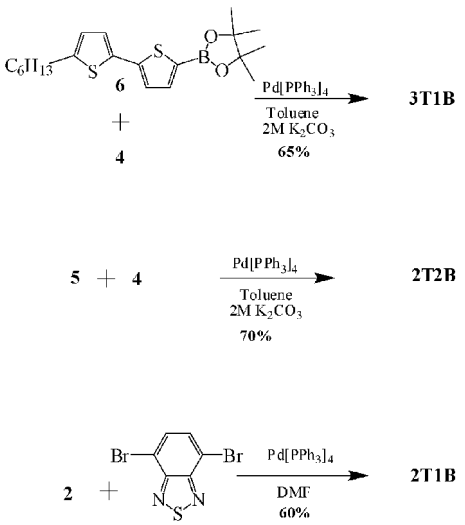

Scheme 3 Synthesis of thiophene–benzothiadiazole (D–A–D) materials.

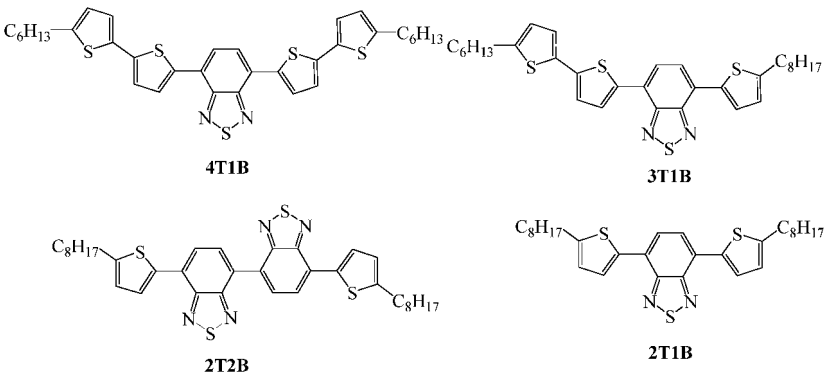

Scheme 1 Chemical structures of thiophene–benzothiadiazole based donor–acceptor–donor (D–A–D) materials.

the catalyst, KOAc (potassium acetate) as the base and 1,4-dioxane as the solvent at 100 °C for 24 h.

The syntheses of all materials are depicted in Scheme 3. **3T1B** was isolated as a bright red powder in 65% yield from the Suzuki coupling of commercially available 2-(5-(5-hexylthiophen-2-yl)thiophen-2-yl)-4,4,5,5-tetramethyl-1,3,2-dioxaborolane (**6**) and **4** using $Pd(PPh_3)_4$ as a catalyst, and 2M K_2CO_3 as base in toluene. **2T2B** was isolated as a red-orange solid in 70% yield by Suzuki coupling using **5** and **4** under the same conditions as used for **3T1B**. **2T1B** was isolated as a bright orange solid in 60% yield by the Stille coupling of one equivalent 4,7-dibromobenzo[c][1,2,5]thiadiazole with 2.5 equivalents of **2**. All the materials were prepared at the ≈300 mg scale and are soluble in common organic solvents such as toluene, dichloromethane, chloroform and THF. All the materials were confirmed by MALDI-TOF (Fig. S1),† and purity by elemental analysis, ^1H and ^{13}C NMR spectroscopy (Fig. S2–S4).†

2.2 Optical properties

The absorption spectra of the materials were measured in chloroform solutions and are shown in Fig. 1a (Table 1). All the materials exhibit two absorption peaks attributed to thiophene constituent and the charge transfer associated with benzothiadiazole moiety (Table 1). As expected **4T1B**, having the longest conjugation length, exhibits a more red shifted peak absorption value of 521 nm compared to the other materials. Consequently, materials **2T2B** and **2T1B**, having a shorter conjugation length (compared to **4T1B** and **3T1B**) exhibit a more blue shifted absorption maxima of 470 nm. The explanation for these varying optical values are also related to the difference in steric hindrance imparted by the benzothiadiazole–thiophene, thiophene–thiophene and benzothidiazole–benzothidiazole linkages and dihedral angles between two units that seem to affect the planarity of the molecules. For example, **2T2B** has a longer conjugation length than **2T1B**, although it shows a 32 nm blue shift in PL maxima. This is attributed to the twisting of two adjacent benzothiadiazole groups thus causing a disruption in conjugation length and the stabilization of the LUMO by the electron-withdrawing groups. Similar observations are also reported recently for pyridine–benzothiadiazole based co-oligomers.[32] **3T1B** shows an absorption maximum at 489 nm which is 19 nm red shifted compared to **2T2B** and **2T1B**, as expected, this value is in between that of **4T1B**, **2T2B** and **2T1B**.

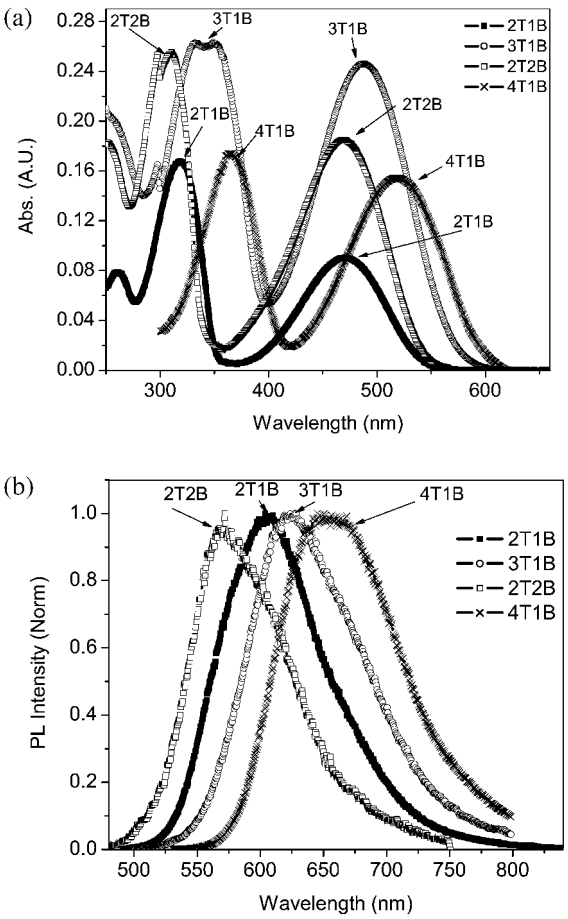

Fig. 1 Absorption (a) and PL (b) spectrum of the materials in chloroform.

The fluorescence spectra for all four materials in chloroform are shown in Fig. 1b (Table 1). **4T1B** and **3T1B** exhibit strong red PL maxima at 650 nm and 628 nm respectively. The blue shift of 22 nm for **3T1B** compared to **4T1B** is due to reduction in conjugation length. **2T2B** and **2T1B** exhibit strong orange emission with PL maxima at 572 nm and 604 nm respectively. The lower band gaps are obtained for **4T1B** and **3T1B** (1.95–2.03 eV) whereas **2T2B** and **2T1B** (2.21–2.25 eV) showed higher band gaps as determined by the optical UV onset values (see Table 1). This result clearly indicates that the donor and acceptor interaction either in alternating fashion or discreet blocks within the molecule plays a significant role in modulating planarity and photophysical properties.

2.3 Electrochemical properties

The material's electrochemical properties were investigated by cyclic voltammetry (CV) to estimate the electrochemical band gaps and HOMO/LUMO energy levels as a function of the D/A ratio. All CV measurements were recorded at room temperature with a conventional three electrode configuration consisting of a platinum wire working electrode, a gold counter electrode, and an Ag/AgCl reference electrode under argon. Electrochemical band gaps were calculated from onset potentials of the anodic and cathodic waves (Fig. S5).† The measured potentials were converted to SCE (saturated calomel electrode) and the corresponding ionization potential (IP) and electron affinity (EA) values were derived from the onset redox potentials, based on −4.4 eV as the SCE energy level relative to vacuum ($EA = E_{red\text{-}onset} + 4.4$ eV, $IP = E_{ox\text{-}onset} + 4.4$ eV). The effect of the D/A ratio on the oxidation/reduction onsets and band gaps can be compared by using the values reported in Table 1. From the values it can be seen that the HOMO levels for the series shows a predictable trend – highest to lowest values correspond to the D/A ratio. As the donor (thiophene) content increases in the material with respect to acceptor (benzothiadiazole), the HOMO level rises (see the trend for **4T1B**,[31] **3T1B** and **2T1B**). This is due to the higher number of electron donating moieties which reduces the oxidation onset. LUMO value tuning depends more on the number of acceptor moieties present in the material.

Table 1 Summary of absorption maxima, emission maxima, HOMO/LUMO levels and derived electrochemical band gaps for materials

Materials	Abs. λ_{max}/nm	PL λ_{max}/nm	Optical band gap/eV[a]	HOMO[b]	LUMO[c]	Electrochemical band gap/eV
4T1B	521, 366	650	1.95	5.15	3.25	1.90
3T1B	489, 349	628	2.03	5.27	3.27	2.00
2T2B	470, 310	572	2.21	5.50	3.33	2.17
2T1B	470, 318	604	2.25	5.34	3.12	2.22

[a] Calculated from optical onset. [b] Calculated from oxidation onset against Ag/AgCl (4.4 eV). [c] Calculated from reduction onset against Ag/AgCl (4.4 eV).

Among all compounds, **2T2B** shows the highest LUMO value, this is due to two electron accepting benzothiadiazole units present in the molecule. From the results reported thus far, it is clear that systematic changes in the donor to acceptor ratios can tune the HOMO–LUMO levels. The lower energy gaps observed for all these D–A–D molecules can be attributed to the intramolecular charge transfer from the thiophene to the benzothiadiazole unit. Electrochemical band gaps obtained from HOMO–LUMO differences was found to be in good agreement with the optical band gaps calculated from the UV-vis absorption onset. Finally, the HOMO values of **4T1B** and **3T1B** are suitable for making oxidative stable devices which is prerequisite condition for processing OTFTs.

2.4 Thermal properties

The thermal behaviour of the all materials was determined by repeated heating–cooling cycles using differential scanning calorimetry (DSC) analyses at a heating rate of 10 °C min^{-1}. From DSC, only **4T1B**[31] and **3T1B** exhibit multiple transitions, suggesting the formation of LC phases (Table 2). For example, the DSC thermogram of **4T1B** indicates multiple endothermic peaks at 125, 175, 202 and 210 °C while **3T1B** shows two endothermic peaks at 105 and 130 °C (Fig. S7).† The lower transition temperatures of **3T1B** compared to **4T1B** is likely due to the increased alkyl chain length, reduced conjugation length, and asymmetric nature of the molecule in terms of aromatic and aliphatic moieties. The other materials in this study, **2T2B** and **2T1B** exhibit only single melting point transitions at 102 and 77 °C respectively (Fig. S6).†

LC behavior was confirmed by using polarized optical microscopy (POM) with a variable temperature hot-stage (Fig. S8).† The optical micrograph for **4T1B** clearly indicates a crystalline to LC transition at 175 °C and LC to isotropic transition at 210 °C on heating. On cooling, the isotropic liquid droplets appear at 195 °C and eventually coalesce into a mosaic structure at 185 °C. In the case of **3T1B**, the optical image shows a crystalline to LC transition at 105 °C and LC to isotropic transition at 130 °C on heating. All of these transitions are consistent with the endothermic peaks observed *via* DSC. It is interesting to note that the same two materials (**3T1B** and **4T1B**) that show LC behaviour also show OTFT mobilities, as will be shown in the OTFT section below. Thermal decomposition of all the materials was carried out using thermogravimetric analysis (TGA). Thermal decomposition temperatures (*T*d, 5% wt loss) for **4T1B**,[31] **3T1B**, **2T2B** and **2T1B** were observed at 390, 350, 340 and 300 °C respectively (Table 2 and Fig. S9).† These values clearly indicate the high thermal stability of the materials which is necessary for various processing methods such as thermally induced vacuum deposition.

Table 2 Summary of melting points and DSC/TGA transition temperature data for materials

Materials	*T*m/°C[a]	*T*c/°C[b]	*T*d/°C[d]
4T1B	175	210	390
3T1B	105	130	350
2T2B	102[c]	—	340
2T1B	77[c]	—	300

[a] Crystal-to-liquid crystal transition temperature. [b] Liquid crystal-to-isotropic transition temperature. [c] Melting point. [d] Decomposition temperature.

2.5 Morphological properties

A solution of each material having a concentration of 0.1 mg ml^{-1} in toluene or tetrahydrofuran was deposited on the substrate using a micro syringe and left to evaporate for up to 48 h in a solvent-saturated atmosphere. This choice of solvents was motivated by the fact that they are good solvents for the four materials. In this way, the morphology of the thin layer deposits are expected to be governed by the self-assembling behavior of the materials (if self-assembly occurs). Thin solid-state deposits from conjugated compounds molecularly dispersed in solution, upon slow evaporation, mainly show three types of interactions (molecule–molecule, molecule–solvent, and molecule–surface), which provides additional tunability for the controlled formation of conjugated nanostructures.[33]

Fig. 2 illustrates the typical morphologies observed by AFM on mica substrate for the four compounds. The two longest molecules, *i.e.*, those with four and five heteroaromatics, **3T1B** and **4T1B** show micrometer-long strip-like structure and more elongated organized monolayers respectively. In contrast, the shortest materials **2T2B** and **2T1B** form round-shaped and non-textured aggregates suggesting that the molecules interact only weakly during the evaporation process. The difference in behavior between the four compounds most probably originates from their different capability of forming densely-packed assemblies of π–π interacting molecules due to intermolecular interactions. The general shape of the molecules, the length of the conjugated backbones, the ratio between the number of thiophene and benzothiadiazole units and therefore their relative affinity to self-assemble are the main parameters governing the long range organization. The observed difference between the measured thicknesses and the calculated values (from molecular

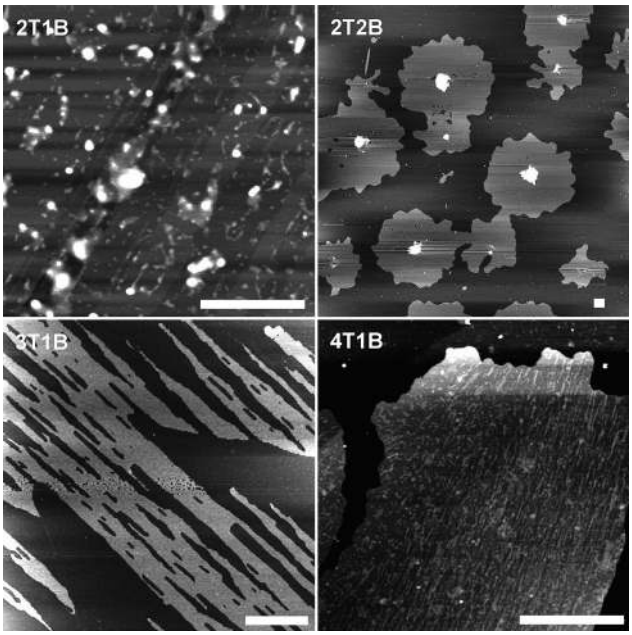

Fig. 2 AFM height images of thin deposits (from toluene solution) (a) **2T1B** (b) **2T2B** (c) **3T1B** and (d) **4T1B** on freshly cleaved mica substrates. The scale bar is 1.0 μm and the *Z*-greyscales are 10 nm for **2T1B** and 5 nm for the others.

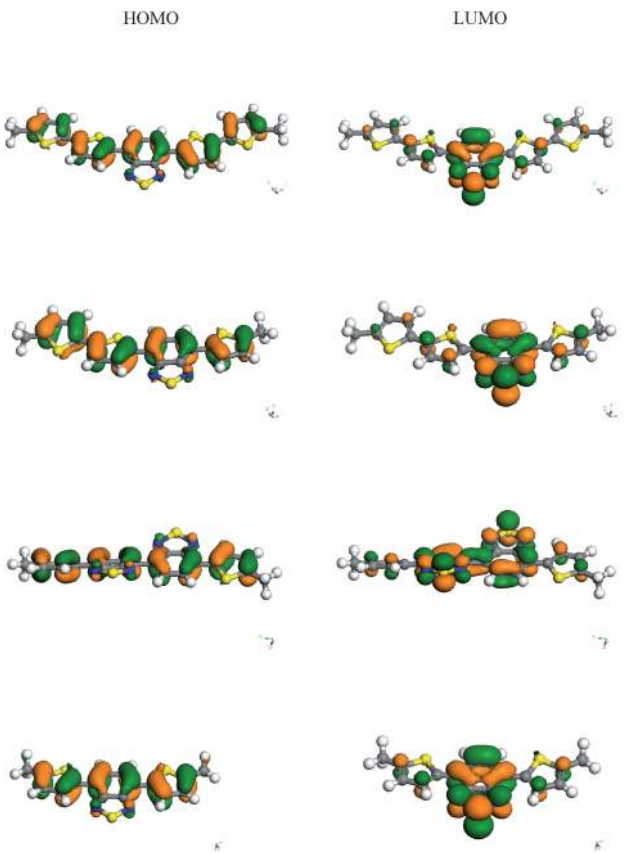

Fig. 3 The electron density isocontours of HOMO and LUMO of materials optimized with DMol[3] Module. The hexyl/octyl groups have been replaced with methyl groups in the calculation.

modeling) for the material length most likely originates from the chemical structures of the compounds. More specifically, the fact that the torsional barrier energies between the thiophene–thiophene, benzothiadiazole–benzothiadiazole and thiophene–benzothiadiazole units are different, leads to a certain capability for the conjugated moieties to rotate and accommodate each other or not. As a consequence, depending on the molecules, the hexyl/octyl chains are pointing in different directions, which therefore affects the packing of the materials. This situation is similar to what it is observed in thiophene–fluorene- and thiophene–indenofluorene-based materials.[34] Layers are sometimes stacked, as shown in Fig. 3b. In this case, when the solvent evaporates slowly, the thin liquid layer dewets and the self-assembly occurs in the round-shaped droplets. The upper monolayers here seen as bright spots in the center of the domains are formed at the end of the self-assembly process. Such kind of observations were also observed for thiophene-based materials.[35] These results show that the supramolecular organization of the different conjugated segment within the chains of D–A–D materials and their relative position seem to be particularly important to achieve efficient π-stacking and good performances in OTFTs.

2.6 Thin film X-ray diffraction

To investigate the molecular packing of D–A–D materials, we performed X-ray diffraction (XRD) experiments of the spin coated thin films deposited on Si/SiO_2 substrates at room temperature. X-Ray diffraction pattern (Fig. S10) with reflections and their corresponding *d*-spacings listed in Table 3. XRD data shows that the high order of crystallinity for materials **4T1B** and **3T1B** is consistent with the LC properties observed in the DSC (see supporting information)† and AFM analysis (Fig. 3) respectively. Lower *d*-spacing (26.58 Å) is observed for the smaller molecule **2T1B**, and higher *d*-spacing (33.43 Å) for the longer molecule **4T1B**. For **4T1B**, a detailed XRD study is described in our previous publication.[31] In the case of **3T1B**, peaks at 3.02 and 3.56 degrees 2θ ($d_{spacing}$ of 29.22 Å and 24.78 Å) indicates that the sample is consistent with the molecular length, which is estimated to be *ca.* 29 Å. For **2T2B** and **2T1B**, peaks at 2.83 and 3.32 degrees 2θ corresponding to $d_{spacing}$ of 31.18 and 26.58 Å respectively. The peak found at 7.72 degrees 2θ is an artifact of the substrate and can be seen only in low intensity samples (**T4B1**, **T2B2** and **T2B1**) whereas for high intensity sample (**3T1B**) the peak is buried in the baseline noise. The higher molecular length of **2T2B** over **3T1B** (confirmed theoretically as well as experimentally) is due to two octyl chain substitution at the both ends of molecule and two benzothiadiazole units. The sharp and strong reflection peak intensities of **3T1B** compared to **4T1B** in solution processed films indicates the high degree of

Table 3 *d*-Spacing calculated from 2θ diffraction peaks of spin coated materials on Si/SiO_2

Materials	2θ (degree)	$d_{spacing}$/Å
4T1B	2.64	33.42
3T1B	3.56, 3.02	29.22, 24.78
2T2B	2.83	31.18
2T1B	3.32	26.58

ordering, often times necessary for achieving high OTFT mobilities.

2.7 DFT electronic structure calculation

To understand the optical/electrochemical trends observed due to the combination of donor and acceptor moieties, density functional theory (DFT) electronic structure computation were performed using the DMol^3 module in the Materials Studio Modeling software package (Accelrys Inc.). Self consistent-field (SCF) density convergence was 10^{-6} and an orbital cutoff of 4 Å was used for all atoms. The convergence tolerances for energy change, maximum force, and maximum displacement between optimization cycles were set as 10^{-5} hartree, 0.002 hartree Å^{-1}, and 0.005 Å, respectively. The electron density isocontours of HOMO/LUMO levels for D–A–D materials are shown in Fig. 3 where hexyl/octyl groups were replaced by the methyl group for simplicity. In all materials, the HOMOs and LUMOs are nearly completely localized on the donor (thiophene) and acceptor (benzothiadiazole) moieties respectively. The localization of the HOMO is higher in **4T1B** and **3T1B** whereas localization of the LUMO is higher in **2T2B** and **2T1B**. Such localization of the HOMO/LUMO orbitals on D/A units has been commonly observed in previous theoretical studies of D–A–D molecules.[36] It is generally indicative of a HOMO → LUMO absorption transition bearing a significant charge-transfer character. The calculated HOMO/LUMO eigen-values of the energy optimized structures are listed in Table 4. The theoretically predicted HOMO energy levels are about 0.6 eV lower whereas the LUMO energy levels match well with electrochemical data. The lower HOMO values than those estimated experimentally may be related with various effects such as conformation and solvation which were not taken into account. The predicted band gap calculated from DFT calculations and optical-electrochemical data shows similar trends. Weak and strong hydrogen bonding due to sulfur and nitrogen within D–A–D oligomers makes possible the minimization of dihedral angles between adjacent (thiophene and benzothiadiazole) units. The **2T2B** molecule is not planar as it showed the distortion and the dihedral angle about 25 degrees measured between two benzothiadiazole units. This observation also supports the blue shift observed in the optical analysis of **2T2B** compared to the other molecules. As the conjugated aromatic part plays a crucial role for the charge delocalization; molecular length of the aromatic portion of these D–A–D materials were determined and their corresponding values are indicated in Table 4. **4T1B** is the longest material and shows a conjugated molecular length around 18.17 Å whereas the molecular lengths for the other materials **3T1B**, **2T2B** and **2T1B** are 14.43, 15.17 and 10.72 Å respectively. **2T2B** shows longer molecular length than **3T1B** due to bigger size of phenyl rings of two benzothiadiazole units (six membered) compared to the thiophene ring (five membered). More planar **3T1B** and **4T1B** oligomers only showed performance in OTFT devices.

2.8 Thin film transistor characteristics

The electrical properties of the D–A–D materials were investigated by fabricating and evaluating OTFTs using solution processing techniques. Top contact geometry devices were fabricated on heavily doped n$^+$-Si wafers with 200 nm thermally grown SiO_2 substrates. The effect of surface modification on device performance using octyltrichlorosilane (OTS-8) self assembled monolayers (SAMs) was also studied. Among all the materials studied here, only the two LC materials **3T1B** and **4T1B** showed OTFT performance. This could be related with various parameters such as appropriate molecular length, packing and favorable arrangements required for the charge carrier transport.

We have previously reported the detailed OTFT device characteristics of **4T1B** using *vacuum processed* films,[31] whereas in this paper we are focussing more on solution processing OTFT device results of new compound **3T1B** and its comparison with **4T1B**. Typical TFT transfer characteristics for **3T1B** and **4T1B** are shown in Fig. 4. The charge carrier mobilities were calculated from the saturation regime of the OTFT transfer characteristics from eqn 1.

$$\mu_{sat} = \left.\frac{\partial I_d}{\partial V_g}\right|_{V_d=\text{const}} \frac{L}{WC_{ins}\left(V_g - V_T\right)} \quad (1)$$

The **3T1B** and **4T1B** based OTFT devices exhibit hole mobilities of 2×10^{-2} cm^2 V^{-1} s^{-1} and 4×10^{-3} cm^2 V^{-1} s^{-1} on bare Si/SiO_2 substrate, respectively. These are the highest mobilities reported for solution processed donor–acceptor–donor (D–A–D) based molecules.[23d] The higher mobility of **3T1B** compared to that of **4T1B** is likely related to the higher molecular ordering shown in XRD films on Si/SiO_2 (strong reflection intensity) and AFM morphology. High charge carrier mobility of **3T1B** is also correlated with asymmetric substitution of alkyl chains for better molecular ordering and alkyl interdigitation. Such kinds of observations have been reported before.[37] Interestingly, SAM treated substrates using OTS-8 improves hole mobility from 4×10^{-3} cm^2 V^{-1} s^{-1} (on bare substrates) to 6×10^{-3} cm^2 V^{-1} s^{-1} (on SAM substrates) for **4T1B** but it does not show any significant improvement in device performance of **3T1B**. The devices of **4T1B** on Si/SiO_2 substrates exhibit noticeable low threshold voltage ($V_T \sim 1.6$ V) compared to **3T1B** devices ($V_T \sim 20$ V).

From these observations it is clear that the donor–acceptor approach can be successfully used to synthesize potential materials for solution processable high mobility OTFT devices.

Table 4 Summary of DFT derived HOMO and LUMO energies and molecular length of conjugated part of the materials

Materials	HOMO/eV	LUMO/eV	E gap/eV	Molecular length of aromatic part/Å
4T1B	−4.59	−3.40	1.18	18.00
3T1B	−4.68	−3.38	1.30	14.36
2T2B	−4.89	−3.50	1.38	15.16
2T1B	−4.82	−3.34	1.48	10.67

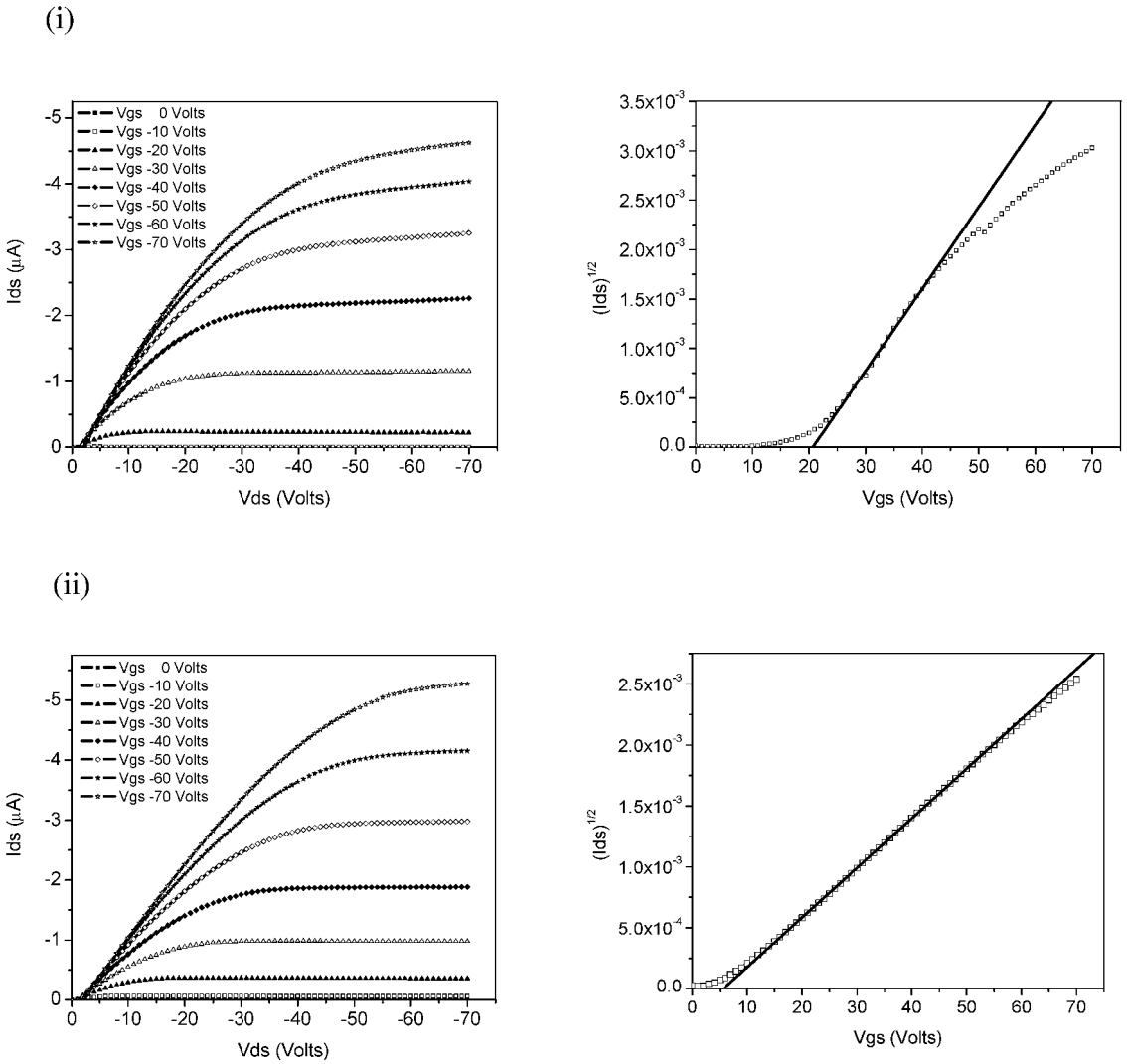

Fig. 4 Current–Voltage I_{ds}–V_{ds}, and I_{ds}–V_{gs}, characteristics of (i) **3T1B** on bare Si/SiO_2 and (ii) **4T1B** on OTS treated substrate.

3. Conclusions

A series of donor–acceptor–donor (D–A–D) materials of thiophene with benzothiadiazole using different D/A ratios have been synthesized and their optical, electrochemical, thermal and thin film transistor properties were compared. Optical spectra of these materials imply that the introduction of electron accepting benzothiadiazole unit in combination with electron donating thiophene reduces the optical band gap up to 1.95 eV. Electrochemical data suggests the fine tuning of HOMO–LUMO values depends on D/A ratio combination and conjugation length of the materials. HOMO values indicate that these D–A–D materials are chemically stable and suitable for making devices. Thermal and optical micrograph analysis of **3T1B** and **4T1B** shows the liquid crystalline behaviour with high ordering in XRD and AFM thin films on Si/SiO_2 substrates. OTFT devices fabricated using **3T1B** and **4T1B** liquid crystalline materials have shown promising charge carrier mobility of 2×10^{-2} cm^2 V^{-1} s^{-1} and 4×10^{-3} cm^2 V^{-1} s^{-1} on bare Si/SiO_2 using simple solution processing techniques. These classes of D–A–D materials are suitable for making even higher mobility solution processable OTFT devices with further optimization. Further synthesis and studies of using various donor–acceptors blocks based materials are in progress in our laboratory.

4. Experimental

4.1. Materials

All commercially available materials were used as received unless otherwise noted. All reactions were carried out using Schlenk techniques under an argon or nitrogen atmosphere in anhydrous solvents.

4.2. Characterization

^1H and ^{13}C NMR data were acquired on a Bruker DPX 400 MHz spectrometer with chemical shifts referenced to residual $CHCl_3$ in $CDCl_3$. Matrix assisted laser desorption/ionization time-of-flight (MALDI-TOF) mass spectra were obtained on a Bruker Autoflex TOF/TOF instrument using dithranol as a matrix with selected ionization salts when required. Differential scanning calorimetry (DSC) was carried out under nitrogen on a TA

Instrument DSC Q100 instrument (scanning rate of 10 °C min^{-1}). Thermogravimetric analysis (TGA) was carried out using a TA Instrument TGA Q500 instrument (heating rate of 10 °C min^{-1}). Cyclic voltammetry experiments were performed using an Autolab potentiostat (model PGSTAT30) by Echochimie. UV-Vis spectra were recorded on a Shimadzu model 2501-PC. Photoluminescence (PL) spectra were measured on a Perkin-Elmer (LS50B) spectrofluorimeter. The photo-micrographs of the materials were taken using a Nikon OPTIPHOT2-POL polarizing optical microscope fitted with a hot stage using a TP-93 temperature programmer and a TMC-6 RGB 1/2″ color CCD camera with net 500X magnification. The sample was placed on a glass slide, covered with a glass coverslip and heated on the hot stage at 10 °C min^{-1} and cooled at 5 °C min^{-1}. All the images have a scale bar of 50 μm. AFM measurements were performed on thin material deposits obtained by solvent casting on glass, silicon or freshly-cleaved mica substrates. These surfaces are very flat, which precludes any influence of the substrate topography on the observed morphology. AFM images were recorded with a Nanoscope V microscope (Veeco Inc., Santa Barbara, CA) operated in tapping mode at room temperature in air, using microfabricated cantilevers (spring constant of 30 N m^{-1}). The images were recorded with 1024 pixel resolution in each direction and are shown as captured. X-ray diffraction patterns of spin coated thin films using equal concentrations deposited at room temperature on the Si/SiO_2 substrates were obtained with a PANalytical X'PERT PRO system using Cu K_α source in air.

4.3. OTFT fabrication and characterization

Top contact organic thin film transistors (OTFTs) were fabricated on heavily doped n^+-Si wafers with 200 nm thermally grown SiO_2. The effect of surface modifications on device performance using OTS-8 SAMs on Si/SiO_2 was studied. OTS-8 treated substrates were obtained by immersing Si/SiO_2 substrates in 0.1 M solution of OTS-8 in toluene at 60 °C for 20 min, and subsequently rinsed by toluene and isopropanol.[38] For all sets of OTFTs, thin films of **T3B1** and **T4B1** were spun cast from 12 mg ml^{-1} solution in chloroform with spin speeds of 1200 rpm for 60 s. Patterned gold layers of thickness ~ 100 nm were deposited for source (S) and drain (D) electrodes through a shadow mask. For a typical OTFT devices reported here, the source–drain channel length (L) and channel width (W) was 100 μm and 3 mm, respectively. The device characteristics of the OTFTs were measured at room temperature under nitrogen with a Keithley 4200 parameter analyzer.

4.4. Synthetic procedures

4.4.1. 4-(5-octylthiophen-2-yl)benzo[c][1,2,5]thiadiazole (3). Tributyl(5-octylthiophene-2-yl)stannane (**2**) (5.0 g, 10.28 mmol), 4-bromobenzo[c][1,2,5]thiadiazole (1.72 g, 8 mmol) and $Pd(PPh_3)_4$ (0.2 mmol, 0.231 mg) were added to a round bottom Schlenk flask and kept under vacuum for 15 min. DMF (30 ml) was then added in to the above mixture under argon and stirred for another 15 min. The solution was subjected to three vacuum/argon refill cycles and then heated at 100 °C with vigorous stirring for 72 h under argon. Reaction completion was confirmed by MALDI-TOF and TLC. The mixture was then poured into water and extracted with dichloromethane. The organic layer was washed three times with water and dried over $MgSO_4$. The crude product was purified using column chromatography (silica gel, hexane : dichloromethane as eluent) to yield 1.72 g (65%) of the product as a dark yellow viscous liquid which solidified at room temperature after a few hours.

δ_H (400 MHz, $CDCl_3$): 7.93–7.92 (d, 1H, Btz), 7.86–7.84 (d, 1H, Btz), 7.74–7.74 (d, 1H, Btz), 7.58–7.56 (d, 1H, Th), 6.87–6.86 (d, 1H, Th) 2.89–2.85 (t, 2H, CH_2), 1.76–1.73 (t, 2H, CH_2), 1.33–1.28 (m, 10H, $5CH_2$), 0.90–0.87 (t, 3H, CH_3).

δ_C (100 MHz, $CDCl_3$): 155.98, 152.59, 148.30, 137.03, 129.98, 128.40, 128.27, 125.54, 125.05, 119.81, 32.24, 31.99, 30.66, 29.71, 29.58, 29.55, 23.02, 14.43.

4.4.2. 4-bromo-7-(5-octylthiophen-2-yl)benzo[c][1,2,5]thiadiazole (4). A solution of *N*-bromosuccinimide (NBS) (1.48 g, 8.31 mmol) in DMF (10 ml) was added dropwise to a solution of (**3**) (2.20 g, 6.65 mmol) with exclusion of ambient light and the reaction mixture was stirred for 72 h at 60 °C. The mixture was poured into water and extracted with dichloromethane. The organic extract was dried over magnesium sulfate and the solvent removed under reduced pressure. The crude product was purified by column chromatography eluting with hexane : dichloromethane to give the product (**4**) (1.75 g, 64%) as bright deep yellow solid.

δ_H (400 MHz, $CDCl_3$): 7.93–7.92 (d, 1H, Btz), 7.83–7.81 (d, 1H, Btz), 7.64–7.62 (d, 1H, Th), 6.87–7.86 (d, 1H, Th), 2.89–2.85 (t, 2H, CH_2), 1.74–1.72 (t, 2H, CH_2),1.32–1.28 (m, 10H, $5CH_2$), 0.88–0.86 (t, 3H, CH_3).

δ_C (100 MHz, $CDCl_3$): 154.25, 152.26, 148.94, 136.27, 132.66, 128.58, 127.94, 125.73, 125.45, 111.96, 32.23, 31.94, 30.68, 29.69, 29.56, 29.54, 23.01, 14.41

4.4.3. 4-(4,4,5,5-tetramethyl-1,3,2-dioxaborolan-2-yl)-7-(5-octylthiophen-2-yl)benzo[c][1,2,5]thiadiazole (5). A solution of **4**(1.10 g, 2.68 mmol), bis(pinacolato)diboron (0.800 g, 3.12 mmol), $PdCl_2$(dppf) (400 mg, 0.48 mmol), and KOAc (0.770 g, 7.7 mmol) in degassed 1,4-dioxane (15 ml) was stirred at 80 °C overnight under argon. The reaction was quenched by adding water, and the resulting mixture was washed with ethyl acetate. The organic layers were washed with brine, dried over Na_2SO_4, and concentrated in vacuum to yield a dark red viscous liquid. The crude product was purified by silica gel chromatography using 3% ethyl acetate in hexane to give the desired compound as a red viscous liquid (0.700, 57%).

δ_H (400 MHz, $CDCl_3$): 8.16–8.14 (d, 1H, Btz), 8.02–8.01 (d, 1H, Btz), 7.78–7.76 (d, 1H, Th), 6.88–6.87 (d, 1H, Th), 2.88–2.86 (t, 2H, CH_2), 1.74–1.72 (t, 2H, CH_2),1.44–1.41 (s, 12H, $4CH_3$), 1.32–1.24 (m, 10H, $5CH_2$) 0.89–0.86 (t, 3H, CH_3).

δ_C (100 MHz, $CDCl_3$): 158.57, 152.31, 149.26, 139.51, 137.11, 133.33, 130.90, 130.05, 129.03, 128.71, 125.71, 124.28, 84.64, 32.24, 31.99, 30.72, 30.06, 29.71, 29.54, 25.30, 23.02, 14.44.

4.4.4. 4-(5-(5-hexylthiophen-2-yl)thiophen-2-yl)-7-(5-octylthiophen-2-yl)benzo[c][1,2,5]thiadiazole (3T1B). Compound **4** (0.600 g, 1.46 mmol) and 2-(5-(5-hexylthiophen-2-yl)thiophen-2-yl)-4,4,5,5-tetramethyl-1,3,2-dioxaborolane (**6**) (0.689 g, 1.83 mmol, 1.26 equiv.), and $Pd(PPh_3)_4$ (42 mg, 0.036 mmol) were added to a 50 ml Schlenk flask and subjected to three vacuum/

argon refill cycles. Argon degassed toluene (12 ml) and aqueous 2 M K_2CO_3 (7 ml) were added to the above mixture and stirred for 10 min under argon. After three vacuum/argon cycles the mixture was heated at 80 °C for 24 h then monitored *via* TLC for reaction completion. Toluene was removed using a rotovap and the product extracted with dichloromethane, then successively washed with water, and dried over $MgSO_4$. Removal of the solvent afforded the crude product which was then purified using column chromatography (silica gel, hexane : dichloromethane as eluent) gives the product as dark orange crystalline solid (0.550 g, 65%).

δ_H (400 MHz, $CDCl_3$): 8.02–8.01 (d, 1H, Btz), 7.95–7.94 (d, 1H, Btz) 7.81–7.79 (dd, 2H, Th), 7.19–7.18 (d, 1H, Th), 7.10–7.09 (d, 1H, Th), 6.87–6.86 (d, 1H, Th), 6.72–6.71(d, 1H, Th), 2.88–2.79 (t, 4H, $2CH_2$), 1.75–1.70 (t, 4H, $2CH_2$), 1.40–1.29 (m, 16H, $8CH_2$), 0.90–0.88 (t, 6H, $2CH_3$).

δ_C (100 MHz, $CDCl_3$): 153.00, 148.39, 146.37, 139.56, 137.94, 137.19, 135.08, 128.47, 127.93, 126.52, 125.64, 125.57, 125.42, 125.33, 124.17, 124.11, 32.27, 31.96, 30.64, 29.75, 29.62, 29.17, 23.06, 14.44.

Found: C 65.88, H 7.61, N 4.78, S 22.79%; Calculated for $C_{32}H_{38}N_2S_4$: C 66.39, H 6.62, N 4.84, S 22.16%; FD-Mass Spectroscopy calcd for $C_{32}H_{38}N_2S_4$: 578.19. Found: 578.14.

4.4.5. 4-(5-octylthiophen-2-yl)-7-(4-(5-octylthiophen-2-yl)benzo[c][1,2,5]thiadiazol-7-yl)benzo[c][1,2,5]thiadiazole (2T2B). Compound **5** (0.125 g, 0.30 mmol), compound **4** (0.160 g, 0.35 mmol, 1.16 equiv.) and $Pd(PPh_3)_4$ (25 mg, 0.017 mmol) were added to a 50 ml Schlenk flask and kept under vacuum for 15 min. Nitrogen degassed toluene (12 ml) and 2 M K_2CO_3 (7 ml) were added in the above mixture and stirred it for 10 min under argon. Vacuum argon cycles were repeated for three times and the mixture was heated at 80 °C for 24 h then monitored *via* TLC for reaction completion. Toluene was removed using a rotovap and the product extracted with dichloromethane, then successively washed with water, and dried over $MgSO_4$. Removal of the solvent afforded the crude product which was then purified using column chromatography (silica gel, hexane : dichloromethane as eluent) gives the product as orange crystalline solid (0.140g, 70%).

δ_H (400 MHz, $CDCl_3$): 8.41–8.40 (d 2H, Btz), 8.01–8.00 (d, 2H, Btz), 7.97–7.95 (d, 2H, Th), 6.91–6.90 (d, 2H, Th), 2.92–2.88 (t, 4H, $2CH_2$), 1.79–1.75 (t, 4H, $2CH_2$), 1.43–1.30 (m, 20H, $10CH_2$), 0.91–0.87 (t, 6H, $2CH_3$).

δ_C (100 MHz, $CDCl_3$): 154.60, 153.17, 148.79, 137.11, 131.63, 128.41, 128.01, 127.95, 125.68, 125.31, 32.26, 32.01 30.74, 29.74, 29.61, 29.54, 23.05, 14.47.

Found: C 65.69, H 6.40, N 8.60, S 19.16%; Calculated for $C_{36}H_{42}N_4S_4$: C 65.61, H 6.42, N 8.50, S 19.46%; FD-Mass Spectroscopy calcd for $C_{35}H_{42}N_4S_4$: 658.23. Found: 658.19.

4.4.6. 4,7-bis(5-octylthiophen-2-yl)benzo[c][1,2,5]thiadiazole (2T1B). Compound **2** (2.92 g, 6.01 mmol), dibromobenzothiadiazole (0.600 g, 2.04 mmol) and $Pd(PPh_3)_4$ (70 mg, 0.047 mmol) were added to a round bottom Schlenk flask and kept under vacuum for 15 min. 15 ml of DMF was then added in the above mixture under argon and stirred for another 15 min. The solution was subjected to three vacuum/argon refill cycles and was then refluxed with vigorous stirring for 72 h under argon. Reaction completion was confirmed by MALDI-TOF and TLC. The mixture was then poured into water and extracted with dichloromethane. The organic layer was washed 2× with water and dried over $MgSO_4$. The crude product was purified using column chromatography (silica gel, hexane: dichloromethane as eluent) to yield 0.550 g (51%) of the product as bright orange solid.

δ_H (400 MHz, $CDCl_3$): 7.93–7.92 (d, 2H, Btz), 7.76 (d, 2H, Th), 6.87–6.86 (d, 2H, Th), 2.90–2.86 (t, 4H, $2CH_2$), 1.76–1.74 (t, 4H, $2CH_2$), 1.33–1.28 (m, 20H, $10CH_2$), 0.90–0.87 (t, 6H, $2CH_3$).

δ_C (100 MHz, $CDCl_3$) 153.08, 148.14, 137.27, 127.77, 126.23, 125.54, 32.24, 32.00, 30.69, 29.72, 29.58, 29.56, 23.02, 14.42.

Found: C 68.90, H 8.44, N 5.39, S 17.94%; Calculated for $C_{30}H_{40}N_2S_3$: C 68.65, H 7.68, N 5.34, S 18.33%; FD-Mass Spectroscopy calcd for $C_{30}H_{40}N_2S_3$: 524.24. Found: 524.29.

5. Acknowledgements

The authors are grateful to the Visiting Investigatorship Programme (VIP) of the Agency for Science, Technology and Research (A*STAR), Republic of Singapore for financial support. We thank Mr Benjamin Tee, Mr Teck Lip Tam and Mr Poh Chong Lim for discussions and characterization support. M. S. and Ph. L. are "Chargé de Recherches" and "Chercheur Qualifié" from the F.R.S. – F.N.R.S. (Belgium) respectively.

6. References

1 (*a*) K. Müllen and G. Wegner, *Electronic Materials: The Material Approach*, Wiley-VCH, Weinheim, 1998; (*b*) H. S. Nalwa, *Handbook of Advanced Electronic and Photonics Materials and Devices*, Academia, San Diego, 2000; (*c*) J. Roncali, *Chem. Rev.*, 1997, **97**, 173; (*d*) C. D. Dimitrakopoulos and P. R. L. Malenfant, *Adv. Mater.*, 2002, **14**, 99; (*e*) M. Mushrush, A. Facchetti, M. Lefenfeld, H. E. Katz and T. J. Marks, *J. Am. Chem. Soc.*, 2003, **125**, 9414; (*f*) A. Yassar, F. Demanze, A. Jaafari, M. El Idrissi and C. Coupry, *Adv. Funct. Mater.*, 2002, **12**, 699.

2 (*a*) C. R. Newman, C. D. Frisbie, D. A. da Silva, J. L. Brédas, P. C. Ewbank and K. R. Mann, *Chem. Mater.*, 2004, **16**, 4436; (*b*) B. K. Shah, D. C. Neckers, J. M. Shi, E. W. Forsythe and D. Morton, *Chem. Mater.*, 2006, **18**, 603; (*c*) Y. Shirota, *J. Mater. Chem.*, 2000, **10**, 1; (*d*) U. Mitschke and P. Bauerle, *J. Mat. Chem.*, 2000, **10**, 1471; (*e*) C. T. Chen, *Chem. Mater.*, 2004, **16**, 4389.

3 (*a*) M. T. Lloyd, J. E. Anthony and G. G. Malliaras, *Materials Today*, 2007, **10**, 34; (*b*) S. Roquet, A. Cravino, P. Leriche, O. Aleveque, P. Frere and J. Roncali, *J. Am. Chem. Soc.*, 2006, **128**, 3459; (*c*) J. Cremer and P. Bauerle, *J. Mat. Chem.*, 2006, **16**, 874; (*d*) R. de Bettignies, Y. Nicolas, P. Blanchard, E. Levillain, J. M. Nunzi and J. Roncali, *Adv. Mater.*, 2003, **15**, 1939; (*e*) M. R. Wasielewski, *Chem. Rev.*, 1992, **92**, 435; (*f*) M. N. Paddonrow, *Acc. Chem. Res.*, 1994, **27**, 18; (*g*) Z. R. Grabowski, K. Rotkiewicz and W. Rettig, *Chem. Rev.*, 2003, **103**, 3899.

4 (*a*) H. Hoppe and N. S. Sariciftci, *J. Mater. Res.*, 2004, **19**, 1924; (*b*) H. Spanggaard and F. C. Krebs, *Sol. Energy Mater. Sol. Cells*, 2004, **83**, 125; (*c*) H. Hoppe and N. S. Sariciftci, *J. Mater. Chem.*, 2006, **16**, 45; (*d*) B. P. Rand, J. Genoe, P. Heremans and J. Poortmans, *Prog. Photovolt. Res. Appl.*, 2007, **15**, 659; (*e*) E. Bundgaard and F. C. Krebs, *Sol. Energy Mater. Sol. Cells*, 2007, **91**, 954; (*f*) S. Gunes, H. Neugebauer and N. S. Sariciftci, *Chem. Rev.*, 2007, **107**, 1324; (*g*) M. Jorgensen, K. Norrman and F. C. Krebs, *Sol. Energy Mater. Sol. Cells*, 2008, **92**, 686; (*h*) B. C. Thompson and J. M. J. Frechet, *Angew. Chem. Intl. Ed.*, 2008, **47**, 58.

5 (*a*) C. A. Di, G. Yu, Y. Liu and D. Zhu, *J. Phys. Chem. B*, 2007, **111**, 14083; (*b*) K. Takimiya, Y. Kunugi and T. Otsubo, *Chem. Lett.*, 2007, **36**, 578; (*c*) G. Horowitz, *J. Mater. Res.*, 2004, **19**, 1946; (*d*) J. E. Anthony, *Chem. Rev.*, 2006, **106**, 5028.

6 (*a*) A. Facchetti, M. Mushrush, H. E. Katz and T. J. Marks, *Adv. Mater.*, 2003, **15**, 33; (*b*) A. Dodabalapur, H. E. Katz, L. Torsi and R. C. Haddon, *Science*, 1995, **269**, 1560.

7 (*a*) H. Sirringhaus, *Adv. Mater.*, 2005, **17**, 2411; (*b*) M. Matters, D. M. de Leeuw, M. J. C. M. Vissenberg, C. M. Hart, P. T. Herwig, T. Geuns, C. M. J. Mutsaers and C. J. Drury, *Opt. Mater.*, 1999, **12**, 189; (*c*) C. J. Drury, C. M. J. Mutsaers, C. M. Hart, M. Matters and D. M. de Leeuw, *Appl. Phys. Lett.*, 1998, **73**, 108.

8 (*a*) G. Horowitz, *Adv. Mater.*, 1998, **10**, 365; (*b*) F. Garnier, *Acc. Chem. Res.*, 1999, **32**, 209; (*c*) B. A. Jones, M. J. Ahrens, M. H. Yoon, A. Facchetti, T. J. Marks and M. R. Wasielewski, *Angew. Chem. Int. Ed.*, 2004, **43**, 6363; (*d*) H. E. Katz, Z. N. Bao and S. L. Gilat, *Acc. Chem. Res.*, 2001, **34**, 359; (*e*) Y. Shirota and H. Kageyama, *Chem. Rev.*, 2007, **107**, 953; (*f*) J. Roncali, *Chem. Rev.*, 1992, **92**, 711.

9 L. Burgi, M. Turbiez, R. Pfeiffer, F. Bienewald, H. J. Kirner and C. Winnewisser, *Adv. Mat.*, 2008, **20**, 2217.

10 (*a*) S. Ando, J. Nishida, Y. Inoue, S. Tokito and Y. Yamashita, *J. Mater. Chem.*, 2004, **14**, 1787; (*b*) S. Ando, J. Nishida, E. Fujiwara, H. Tada, Y. Inoue, S. Tokito and Y. Yamashita, *Chem. Lett.*, 2004, **33**, 1170; (*c*) S. Ando, J. Nishida, H. Tada, Y. Inoue, S. Tokito and Y. Yamashita, *J. Am. Chem. Soc.*, 2005, **127**, 5336.

11 (*a*) T. Izumi, S. Kobashi, K. Takimiya, Y. Aso and T. Otsubo, *J. Am. Chem. Soc.*, 2003, **125**, 5286; (*b*) T. Takahashi, K. Takimiya, T. Otsubo and Y. Aso, *Org. Lett.*, 2005, **7**, 4313.

12 (*a*) H. Meier, B. Muhling, A. Oehlhof, S. Theisinger and E. Kirsten, *Eur. J. Org. Chem.*, 2006, **2**, 405; (*b*) H. Meier, *Angew. Chem. Int. Ed.*, 2005, **44**, 2482; (*c*) H. Meier, J. Gerold, H. Kolshorn and B. Muhling, *Chem. Eur. J.*, 2004, **10**, 360; (*d*) H. Meier, J. Gerold, H. Kolshorn, W. Baumann and M. Bletz, *Angew. Chem. Int. Ed.*, 2002, **41**, 292.

13 (*a*) Y. Yamaguchi, T. Ochi, T. Wakamiya, Y. Matsubara and Z. Yoshida, *Org. Lett.*, 2006, **8**, 717; (*b*) Y. Yamaguchi, T. Tanaka, S. Kobayashi, T. Wakamiya, Y. Matsubara and Z. Yoshida, *J. Am. Chem. Soc.*, 2005, **127**, 9332; (*c*) C. L. Li, S. J. Shieh, S. C. Lin and R. S. Liu, *Org. Lett.*, 2003, **5**, 1131; (*d*) M. S. Wong, Z. H. Li, Y. Tao and M. D'Iorio, *Chem. Mater.*, 2003, **15**, 1198.

14 (*a*) H. Detert, D. Schollmeyer and E. Sugiono, *Eur. J. Org. Chem.*, 2001, **15**, 2927; (*b*) L. P. Candeias, G. H. Gelinck, J. J. Piet, J. Piris, B. Wegewijs, E. Peeters, J. Wildeman, G. Hadziioannou and K. Müllen, *Synth. Met.*, 2001, **119**, 339; (*c*) B. Strehmel, A. M. Sarker, J. H. Malpert, V. Strehmel, H. Seifert and D. C. Neckers, *J. Am. Chem. Soc.*, 1999, **121**, 1226; (*d*) K. H. Schweikart, M. Hanack, L. Luer and D. Oelkrug, *Eur. J. Org. Chem.*, 2001, **2**, 293; (*e*) S. E. Dottinger, M. Hohloch, J. L. Segura, E. Steinhuber, M. Hanack, A. Tompert and D. Oelkrug, *Adv. Mater.*, 1997, **9**, 233.

15 (*a*) H. A. M. van Mullekom, J. A. J. M. Vekemans, E. E. Havinga and E. W. Meijer, *Mater. Sci. Eng.*, 2001, **32**, 1; (*b*) M. Pomeramtz, *Handbook of Conducting Polymers*, 2nd ed,T. A. Skotheim, R. L. Elsenbaumer and J. R. Reynolds Eds. Marcel Dekker: New York, 1998, 11, 277.

16 (*a*) E. E. Havinga, W. Tenhoeve and H. Wynberg, *Polym. Bull.*, 1992, **29**, 119; (*b*) E. E. Havinga, W. Tenhoeve and H. Wynberg, *Synth. Met.*, 1993, **55**, 299; (*c*) S. Tanaka and Y. Yamashita, *Synth. Met.*, 1997, **84**, 229.

17 M. Jayakannan, P. A. Van Hal and R. A. J. Janssen, *J. Polym. Sci. Part A: Polym. Chem.*, 2002, **40**, 251.

18 Y. S. Park, D. Kim, H. Lee and B. Moon, *Org. Lett.*, 2006, **8**, 4699.

19 H. A. M. van Mullekom, J. A. J. M. Venkemans and E. W. Meijer, *Chem. Eur. J.*, 1998, **4**, 1235.

20 J. M. Hancock, A. P. Gifford, Y. Zhu, Y. Lou and S. A. Jenekhe, *Chem. Mater.*, 2006, **18**, 4924.

21 T. Kono, D. Kumaki, J. Nishida, T. Sakanoue, M. Kakita, H. Tada, S. Tokito and Y. Yamashita, *Chem. Mater.*, 2007, **6**, 1218.

22 H. Moon, W. S. Jahng and M. D. Curtis, *J. Mat. Chem.*, 2008, **18**, 4856.

23 (*a*) H. E. Katz, A. Dodabalapur, L. Torsi and D. Elder, *Chem. Mater.*, 1995, **7**, 2238; (*b*) F. Garnier, A. Yassar, R. Hajlaoui, G. Horowitz, F. Deloffre, B. Servet, S. Ries and P. Alnot, *J. Am. Chem. Soc.*, 1993, **115**, 8716.

24 (*a*) M. Funahashi, F. P. Zhang and N. Tamaoki, *Adv. Mater.*, 2007, **19**, 353; (*b*) M. Funahashi and J. Hanna, *Adv. Mater.*, 2005, **17**, 594; (*c*) R. Azumi, G. Gotz and P. Bauerele, *Syn. Met.*, 1999, **101**, 544; (*d*) M. Melucci, L. Favaretto, C. Bettini, M. Gazzano, N. Camaioni, P. Maccagnani, P. Ostoja, M. Monari and G. Barbarella, *Chem Eur. J.*, 2007, **13**, 10046.

25 K. Oikawa, H. Monobe, K. Nakayama, T. Kimoto, K. Tsuchiya, B. Heinrich, D. Guillon, Y. Shimizu and M. Yokoyama, *Adv. Mater.*, 2007, **19**, 1864.

26 (*a*) M. Karikomi, C. Kitamura, S. Tanaka and Y. Yamashita, *J. Am. Chem. Soc.*, 1995, **117**, 6791; (*b*) Y. Yamashita, K. Ono, M. Tomura and K. Imaeda, *Chem. Commun.*, 1997, **19**, 1851.

27 (*a*) M. T. S. Ritonga, H. Sakurai and T. Hirao, *Tetrahedron Lett.*, 2002, **43**, 9009; (*b*) B. A. D. Neto, A. S. A. Lopes, G. Ebeling, R. S. Goncalves, V. E. U. Costa, F. H. Quina and J. Dupont, *Tetrahedron*, 2005, **61**, 10975; (*c*) Y. Yamashita, K. Suzuki and M. Tomura, *Synth. Met.*, 2003, **133**, 341.

28 (*a*) M. Akhtaruzzaman, N. Kamata, J. Nishida, S. Ando, H. Tada, M. Tomura and Y. Yamashita, *Chem. Commun.*, 2005, **25**, 3183; (*b*) M. Zhang, H. N. Tsao, W. Pisula, C. D. Yang, A. K. Mishra and K. Müllen, *J. Am. Chem.Soc.*, 2007, **129**, 3472; (*c*) J. Zaumseil, C. L. Donley, J. S. Kim, R. H. Friend and H. Sirringhaus, *Adv. Mater.*, 2006, **20**, 2708.

29 (*a*) M. Svensson, F. L. Zhang, S. C. Veenstra, W. J. H. Verhees, J. C. Hummelen, J. M. Kroon, O. Inganas and M. R. Andersson, *Adv. Mater.*, 2003, **15**, 988; (*b*) E. Bundgaard and F. C. Krebs, *Sol. Energy Mater. Sol. Cells.*, 2007, **91**, 1019; (*c*) E. Bundgaard and F. C. Krebs, *Poly. Bull.*, 2005, **55**, 157; (*d*) D. Muhlbacher, M. Scharber, M. Morana, Z. G. Zhu, D. Waller, R. Gaudiana and C. Brabec, *Adv. Mater.*, 2006, **18**, 2884; (*e*) E. Bundgaard and F. C. Krebs, *Macromolecules*, 2006, **39**, 2823; (*f*) E. Bundgaard, S. E. Shaheen, F. C. Krebs and D. S. Ginley, *Sol. Energy Mater. Sol. Cells.*, 2007, **91**, 1631.

30 In this paper we renamed the previously reported compound DH-BTZ-4T as T4B1.

31 P. Sonar, S. P. Singh, S. Sudhakar, A. Dodabalapur and A. Sellinger, *Chem. Mater.*, 2008, **9**, 3184.

32 M. Akhtaruzzaman, M. Tomura, J. Nishida and Y. Yamashita, *J. Org. Chem.*, 2004, **69**, 2953.

33 M. Surin, P. Leclére, S. de Feyter, M. M. S. bdel-Mottaleb, F. C. de Schryver, O. Henze, W. J. Feast and R. Lazzaroni, *J. Phys. Chem. B*, 2006, **110**, 7898.

34 M. Surin, P. Sonar, A. C. Grimsdale, K. Müllen, R. Lazzaroni and P. Leclére, *Adv. Funct. Mater.*, 2005, **15**, 1426.

35 P. Leclére, M. Surin, P. Brocorens, M. Cavallini, F. Biscarini and R. Lazzaroni, *Mater. Sci. Eng. Rep.*, 2006, **55**, 1.

36 (*a*) N. Acar, J. Kurzawa, N. Fritz, A. Stockmann, C. Roman, S. Schneider and T. Clark, *J. Phys. Chem. A*, 2003, **107**, 9530; (*b*) A. Elangovan, K. M. Kao, S. W. Yang, Y. L. Chen, T. I. Ho and Y. L. O. Su, *J. Org. Chem.*, 2005, **70**, 4460; (*c*) J. A. Marsden, J. J. Miller, L. D. Shirtcliff and M. M. Haley, *J. Am. Chem. Soc.*, 2005, **127**, 2464.

37 (*a*) F. Zhang, M. Funahashi and N. Tamaoki, *App. Phy. Lett.*, 2007, **91**, 063515; (*b*) S. A. Ponomarenko, S. Kirchmeyer, A. Elschner, N. M. Alpatova, M. Halik, H. Klauk, U. Zschieschang and G. Schmid, *Chem. Mater.*, 2006, **18**, 579.

38 B. S. Ong, Y. L. Wu, P. Liu and S. Gardner, *Adv. Mater.*, 2005, **17**, 1141.